



## Density Normal Compaction Trend in the Peciko Field, Lower Kutai Basin, Indonesia

AGUS M. RAMDHAN<sup>1</sup>, NEIL R. GOULTY<sup>2</sup>, STUART J. JONES<sup>2</sup>, and LAMBOK M. HUTASOIT<sup>1</sup>

<sup>1</sup>Department of Geology, Institut Teknologi Bandung, Jln. Ganesha 10, Bandung 40132, Indonesia

<sup>2</sup>Department of Earth Sciences, Durham University, South Road, Durham DH1 3LE, UK

Corresponding author: [agusmr@gl.itb.ac.id](mailto:agusmr@gl.itb.ac.id)

Manuscript received: January, 13, 2020; revised: February, 02, 2020;

approved: February, 24, 2020; available online: September, 21, 2020

**Abstract** - The density normal compaction trend is the mandatory parameter in order to calculate contribution of disequilibrium compaction to overpressure, in the presence of unloading to total overpressure. In this paper, mudrock compaction behaviour is studied in the Peciko Field. The density normal compaction trend was constructed in a normally pressured section, where the temperature is <120°C, within the transformation of smectite–illite zone. The compaction trend includes not only vertical effective stress, but also diagenesis, especially smectite-illite transformation, as dependant factor for compaction, both termed as  $\beta$ . This compaction trend is also known as Skempton–Dutta compaction model. Quardros–Linares fifth-order kinetic reaction was found that could model smectite-illite transformation in the studied area fairly well. The plot between  $\beta$  and smectite content shows a very good match, confirming that Skempton–Dutta compaction model is valid for the entire range of smectite-illite transformation. In the area where the density log is unavailable, the density normal compaction can be constructed from temperature history acting as a proxy for smectite-illite transformation, with some local calibration.

**Keywords:** disequilibrium, mudrock, density normal, Lower Kutai Basin, Peciko Field

© IJOG - 2020. All right reserved

### How to cite this article:

Ramdhan, M.R., Goult, N.R., Jones, S.J., and Hutasoit L.M., 2020. Density Normal Compaction Trend in the Peciko Field, Lower Kutai Basin, Indonesia. *Indonesian Journal on Geoscience*, 7 (3), p. 253-265. DOI: [10.17014/ijog.7.3.253-265](https://doi.org/10.17014/ijog.7.3.253-265)

### INTRODUCTION

It is necessary to find a density normal compaction trend for mudstones to estimate pore pressure in overpressured wells using the two-step approach proposed by Goult *et al.* (2016), to be able to calculate the contribution of disequilibrium compaction to total overpressure magnitude, in the presence of unloading overpressuring. In analyzing data from the Bekapai Field, Lower Kutai Basin, to determine the contributions to overpressure due to disequilibrium compaction and unloading mecha-

nisms, Ramdhan and Goult (2018) assumed that illitization of smectite could be modelled as a first-order kinetic reaction, as proposed by Dutta (1986, 2016). However, even in the example selected by Dutta (2016), the predicted trend on the sonic-density crossplot using this model gives a poor fit to the wireline log data in the transition zone between the early compaction trend for smectite-rich mudstone and the late compaction trend for illite-rich mudstone. In the Bekapai wells, the density data were only of good quality below ~2,400 m depth, where the temperatures were

>100°C, so modelling illitization as a first-order kinetic reaction gave satisfactory results because most of the smectite was already illitized at the top of the depth interval analyzed.

Cuadros and Linares (1996) proposed that illitization of smectite could be modelled as a fifth-order kinetic reaction, in spite of the complexity of the sequence of reactions involved. In this study, that model is applied to hydrostatically pressured mudstones in the Peciko Field, where the top of overpressure is at depths greater than 3 km and temperatures of >120°C. Thus, wireline logs are available for analysis from a large thickness of hydrostatically pressured Neogene mudstones across the depth range where transformation of smectite to illite occurs. Generally, the top of overpressure in the Peciko Field is located next to the top of prodelta sequence, while the section analyzed here is far above the prodelta sequence. Lithologically, the sequence is composed monotonously of sand-mudrock intercalations (Ramdhan and Goulty, 2011). Ramdhan and Goulty (2011) also analyzed that it was less likely that the difference between sand and mudrock pressure to present. The absence of thick mudrock interval to hold pressure is different in the section above prodelta shale, and thus pressure measurements in sand in the analyzed section which are hydrostatic can be used to imply mudrock pressures which are also in hydrostatic condition.

The approach is to compare the diagenesis function,  $\beta$ , in the Skempton-Dutta compaction relationship with the relative proportion of smectite modelled as proposed by Cuadros and Linares (1996). The expectation is that  $\beta$  should increase as the smectite content of the mudstones decreases, and the mudstones become more compactable. Following Dutta (2002, 2016), that the relationship between  $\beta$  and the smectite content is assumed linear.

In this paper, satisfactory fits were obtained to the density log for ten Peciko wells by modelling density as a function of vertical effective stress and smectite content as the only variables, which required five constants to be chosen as fitting parameters. In the area where the density log is

poor, this methodology could be applied in order to get a reliable density normal compaction trend to be used to calculate overpressure magnitude generated by disequilibrium compaction.

## GEOLOGICAL SETTING

The Peciko Field is a gas field located on the Median Axis, in the shelfal area, Lower Kutai Basin, Indonesia (Figure 1). The Kutai Basin development has very much been affected by the interactions between Indian-Australian Plate, Eurasia Plate, and Pacific Plate (*e.g.* Hall, 2009). Among the interactions are the opening of the South China Sea to the north, at the margin of the Eurasia Plate, the westward motion of the Pacific Plate, and the northward motion of the Indian-Australian Plate. Cloke *et al.* (1999) and Chambers *et al.* (2004) comprehensively investigated the development of the Kutai Basin. There are four major development phases of the basin as described below.

1. Middle to Late Eocene. Basin initiation marked by the development of half grabens as a consequence of tectonic extension experienced by the Southeast Asia region, including the Kalimantan area (*e.g.* Hall, 2009). This process was accompanied by syn-rift sedimentation.
2. Latest Eocene to Late Oligocene. Sag period marked by a deep marine mudrock sedimentation in the basin centre and carbonate platform development at the basin edge near the basement high.
3. Latest Oligocene to Early Miocene. Early development of deltaic sediments in the Lower Kutai Basin. There are two phases of tectonics related to this development: inversion/uplift and volcanism in the hinterland, followed by a second extensional phase in the basin centre.
4. Middle Miocene to Present. The main inversion stage with development of the Samarinda Anticlinorium, the major anticlinal structure in the Kutai Basin, and progradation of the delta toward the present day Mahakam Delta.

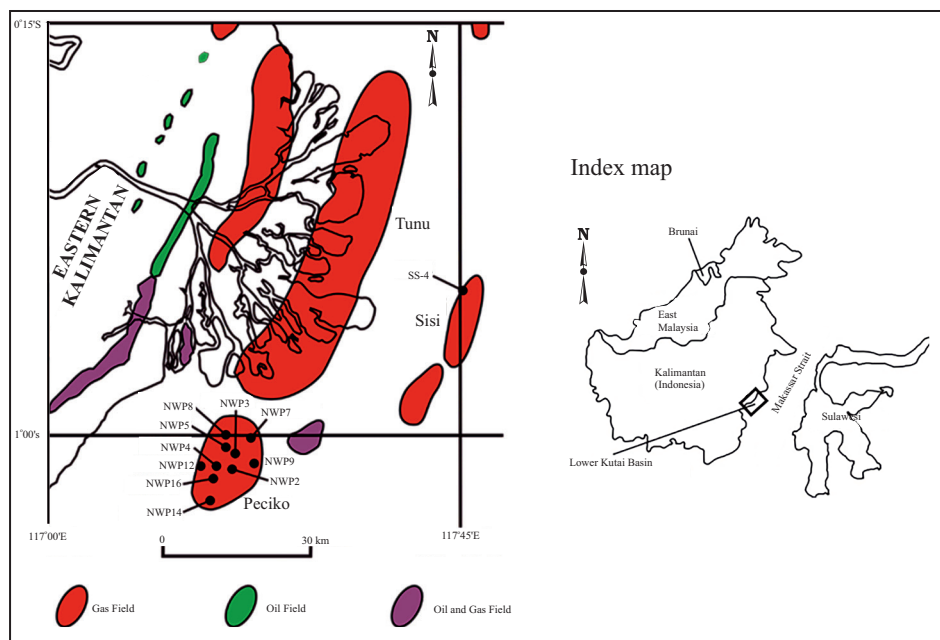


Figure 1. Location map showing wells used in this study.

Ramdhan and Goulty (2010) have summarized the geological evolution of the Peciko Field. The water depth in the Peciko Field is around 40 m. Structurally, this field is an unfaulted anticline and stratigraphically, the productive interval in the Middle–Upper Miocene succession on the Median Axis, including the Peciko Field, is the Tunu Main Zone (Figure 2).

The Tunu Main Zone is subdivided into six intermediate stratigraphic units (SUs), of which only the uppermost five are present in the Peciko Field. They have an average thickness of 300 - 400 m, based on the presence of third-order maximum flooding surfaces (Total E & P Indonesia, 2000). The dominant reservoirs in this field are distributary mouth bars, the dimensions of individual mouth bars are 1 - 3 m thick and 1,500 - 4,000 m wide, and stacked mouth bars attaining thicknesses of 10 - 30 m (Samson *et al.*, 2005). The burial history of the Tunu Main Zone in this field shows that the sedimentation rate during the last 8 Ma has been fairly constant at around 279 - 306 m/Ma (Table 1). Most of the field surrounding Mahakam Delta including Peciko Field is a great place to study mudrock compaction since the sedimentation has been continuous at least during Neogene section, and therefore, the

Neogene mudrocks are in their maximum burial depth at the present time.

The temperature data derived from ten wells shows that the geothermal gradient is ~30°C/km, with the surface temperature of around 30°C (Figure 3). It is also reasonable to assume that the thermal history in the studied area is constant since the sedimentation is continuous and the major tectonic events are absent. Based on this geothermal gradient and the relatively high surface temperature, this part of the Lower Kutai Basin is warm enough for temperature-driven processes such as clay diagenesis (*e.g.* smectite–illite transformation) to take place at a relatively shallow depth.

## THEORETICAL BACKGROUND

### *Skempton-Dutta Compaction Relationship*

The relationship between vertical effective stress ( $\sigma'_v$ ), and void ratio ( $e$ ) for mechanical compaction given by Skempton (1969) is:

$$\sigma'_v = \sigma'_0 \exp(-\beta e) \dots\dots\dots(1)$$

where  $\sigma'_0$  is the vertical effective stress when the void ratio is zero and  $\beta$  is a constant.

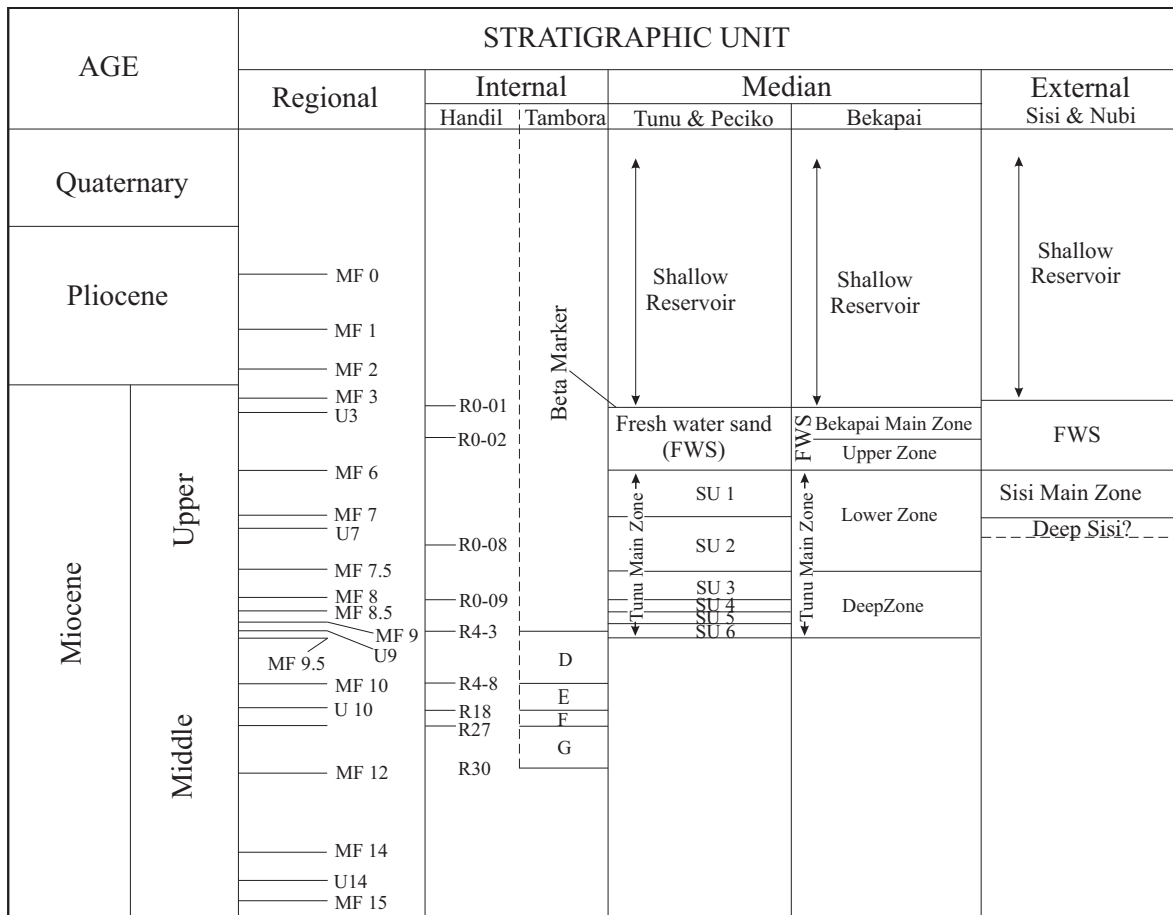


Figure 2. Stratigraphy of the Internal, Median, and External axes of the Lower Kutai Basin, including Peciko Field (Total E&P, 2000).

Table 1. Burial History of the Ten Peciko Wells Used in this Study

Well number	TVDS of the 8 Ma horizon* (m)	Interval of age zero to 8 Ma	
		Thickness (m)	Burial rate (m/Ma)
NWP-2	2270	2230	278.75
NWP-3	2370	2330	291.25
NWP-4	2340	2300	287.5
NWP-5	2440	2400	300
NWP-6	2290	2250	281.25
NWP-7	2490	2450	306.25
NWP-8	2640	2600	325
NWP-9	2480	2440	305
NWP-12	2470	2430	303.75
NWP-14	2380	2340	292.5

Equation 1 was determined empirically by Skempton (1969) from experimental data on clays and, as he pointed out, only applied for values of vertical effective stress that were substantially less than  $\sigma'_0$  because the void ratio must approach

zero asymptotically at high vertical effective stress.

Dutta (1986, 2016) modified Equation 1 by re-defining  $\beta$  as the ‘diagenesis function’ to account for the illitization of smectite according to the

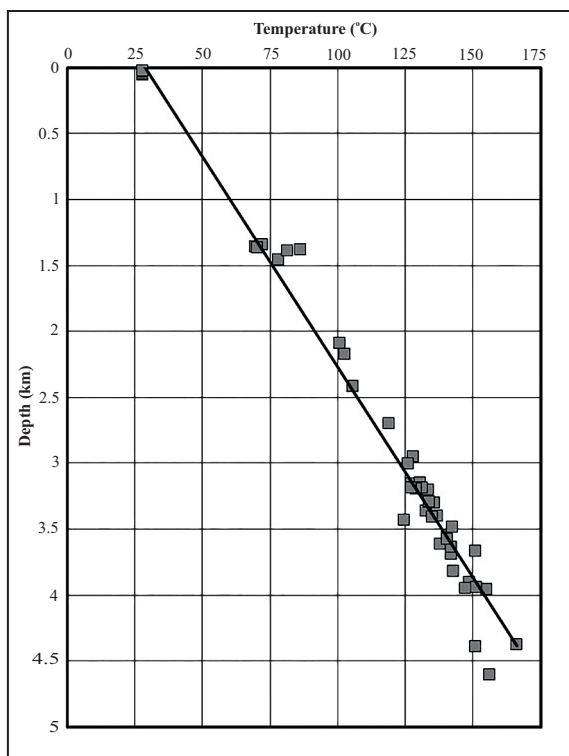


Figure 3. Estimated thermal gradient of 30°C/km plus seabed temperature of 30°C (black line) from temperature measurements of several wells in the Peciko Field (black rectangles).

mudstone temperature history. He then proceeded by assuming that smectite-illite transformation occurred as a first-order kinetic reaction. However any model could be evaluated for illitization of smectite by fitting the predicted smectite fraction to the depth profile of  $\beta$  in hydrostatically pressured mudstones.  $\beta$  may be determined from the density log by rewriting Equation 1 in the form of:

$$\beta = (\ln\sigma'_0 - \ln\sigma'_v)/e \dots\dots\dots(2)$$

Void ratio is obtained from the logged density in mudstone,  $\rho$ :

$$e = (\rho_s - \rho)/(\rho - \rho_f) \dots\dots\dots(3)$$

where  $\rho_s$  is the density of the solid grains, assumed to be 2.75 g cm<sup>-3</sup>, and  $\rho_f$  is the density of the pore fluid, assumed to be 1.0 g cm<sup>-3</sup>. It was necessary to make an assumption to estimate a suitable value of  $\sigma'_0$  for using in Equation 2. Dutta (2016) reported that  $\beta$  asymptotically approached the value 9.4 at great depth, so for the

ten Peciko wells analyzed, the values of  $\sigma'_0$  were determined that gave  $\beta = 9.2$  at the depth where the temperature had reached 120°C, discarded the two extreme values, and averaged the other eight to yield  $\sigma'_0 = 107$  MPa.

**Transformation of Smectite to Illite**

The kinetic of smectite to illite transformation has been studied by previous researchers (*e.g.* Hower *et al.*, 1976; Boles and Frank, 1979; Colten-Bradley, 1987; Cuadros and Linares, 1996). Cuadros and Linares (1996) proposed that the illitization of smectite could be modelled as a fifth-order kinetic reaction:

$$-dS/dt = kK^{0.25} S^5 \dots\dots\dots(4)$$

Where:  $S$  is the proportion of smectite layers in mixed-layer illite-smectite (I-S);  $t$  is time;  $k$  is the rate constant which is dependent on temperature, and  $K$  is the concentration of potassium.

The variable  $K$  was termed the ‘effective potassium concentration’ by Cuadros (2006), because it was affected not only by the concentration of potassium but also by the concentrations of other cations, especially calcium, that compete with potassium for the smectite interlayer sites by ion mobility in the sediments, and possibly by other variables (Robertson and Lahann, 1981; Elliott and Matisoff, 1996; Bjørlykke, 1998).

Cuadros (2006) applied Equation 4 to model illitization in eight wells. He claimed that this kinetic equation allowed an accurate fit to the experimental data in all the wells, reproducing both the illitization onset and the patterns of the plots of smectite fraction versus depth. He obtained an equation for the reaction rate from the experimental data of Cuadros and Linares (1996), who had obtained values at 120°C, 175°C, and 200°C, with an additional assumed value of zero for the reaction rate at 50°C. From these four data values, he determined by least squares the following quadratic equation in temperature for the reaction rate:

$$k = 1.213 \times 10^{-9}T^2 - 6.608 \times 10^{-8}T - 2.033 \times 10^{-7} \dots\dots\dots(5a)$$



with units  $M^{0.25} \text{ days}^{-1}$ , where  $T$  is the temperature in  $^{\circ}\text{C}$ . In Equation 5a,  $k > 0$  for  $T > 57.4^{\circ}\text{C}$ . Given that  $1 \text{ a} = 365.23 \text{ days}$ , this equation can be rewritten as:

$$k = 4.43 \times 10^{-7}T^2 - 2.413 \times 10^{-5}T - 7.425 \times 10^{-5} \dots\dots\dots(5b)$$

with units  $M^{0.25} \text{ a}^{-1}$ , where  $T$  is the temperature in  $^{\circ}\text{C}$ .

The calculated depth profile was compared for smectite fraction with the log-derived depth profile for  $\beta$  and found that Equation 5b gave much too shallow an onset for smectite illitization. By trial and error, the approach of Cuadros (2006) was modified by adding to the three valid experimental data points of Cuadros and Linares (1996) the assumed value of zero for the reaction rate at the temperature of  $66^{\circ}\text{C}$ . Then, the equation for the reaction rate determined by least squares becomes:

$$k = 3.579 \times 10^{-7}T^2 + 1.677 \times 10^{-5}T - 1.906 \times 10^{-3} \dots\dots\dots(6)$$

with units  $M^{0.25} \text{ a}^{-1}$ , where  $T$  is the temperature in  $^{\circ}\text{C}$ . In Equation 6,  $k > 0$  for  $T > 70.7^{\circ}\text{C}$ . At lower temperatures, the reaction rate is set to zero Integrating Equation 4 gives:

$$1/S_f^4 - 1/S_i^4 = 4kK^{0.25}t \dots\dots\dots(7a)$$

where  $S_f$  and  $S_i$  are the final and initial fractions of smectite layers in I-S for a time-step of length  $t$ .

If  $K$  is assumed to be constant for the sequence under investigation, then Equation 7a is equivalent to:

$$1/S^4 = 1/S_0^4 + 4K^{0.25} \int_0^{\tau} k dt \dots\dots\dots(7b)$$

where  $S$  is the fraction of smectitic interlayers remaining in a mudstone of age  $\tau$  and  $S_0$  is the initial fraction of smectite layers.

The proportion of smectite interlayers was calculated from this equation in the form:

$$1/S_n^4 = 1/S_0^4 + 4K^{0.25} \sum_{i=1}^n k_i \dots\dots\dots(7c)$$

where it is assumed that  $K$  is constant, the reaction rate at each depth step  $k_j$  is given by Equation 6, and the time that elapsed while the mudstone was at each depth step  $\Delta t_j$  is obtained from the burial history.

Cuadros (2006) claimed that where the initial rate of illitization was fast enough, it made no significant difference to the calculated fractions of smectite layers at the present day if it was assumed that initially all the layers in I-S were smectite. This claim was tested using values of 0.7 and 1 for  $S_0$ . For each value of  $S_0$ , empirically the value of  $K$  was determined by assuming that  $S \approx 0.23$  at the depth where the temperature had reached  $120^{\circ}\text{C}$ . The justification for this assumption is provided by observations, summarized by Cuadros (2006) as follows: “Data from sedimentary basins where the complete smectite-to-illite transformation has been recorded, the proportion of smectite in I-S decreases little with depth in the shallow sediments, then it decreases abruptly up to a value that has been frequently found to be  $\sim 20\%$ , and finally it decreases slightly or remains constant in the deeper sediments.” The XRD data reported by Clauer *et al.* (1999) from the shelfal area of the Lower Kutai Basin are consistent with this statement.

**DATASET**

Density logs were available from sixteen wells in the Peciko Field. In the shelfal area of the Lower Kutai Basin, the density logs from the Peciko Field are of the best quality, because those wells were drilled with oil-based muds (Ramdhan and Goulty 2010). Six wells were discarded, five because there was no coverage at shallower depths and one because the log is particularly noisy. **The ten wells retained (Figure 1) all had coverage from depths of less than 500 m subsea.** The top of overpressure inferred from RFT measurements in the sandstone beds is at depths greater than 3000 m subsea in all ten wells, apart from some small overpressures attributable primarily to hydrocarbon buoyancy. Hence, the

depth interval for investigation was chosen to be 500 - 3,000 m subsea, corresponding to a temperature range of 45 - 122°C (water depth 40 m, seafloor temperature 30°C, geothermal gradient 30°C /km).

As shown in Figure 4 for Well NWP-2, mudstone data points on the wireline logs were

selected based on both natural gamma response and the difference between neutron porosity and density porosity (NPHI–DPHI). Bounding values of natural gamma response and NPHI–DPHI were chosen independently for each well (dark blue box in Figure 4f), and yielded between 5,000 and 7,000 mudstone data points in each well

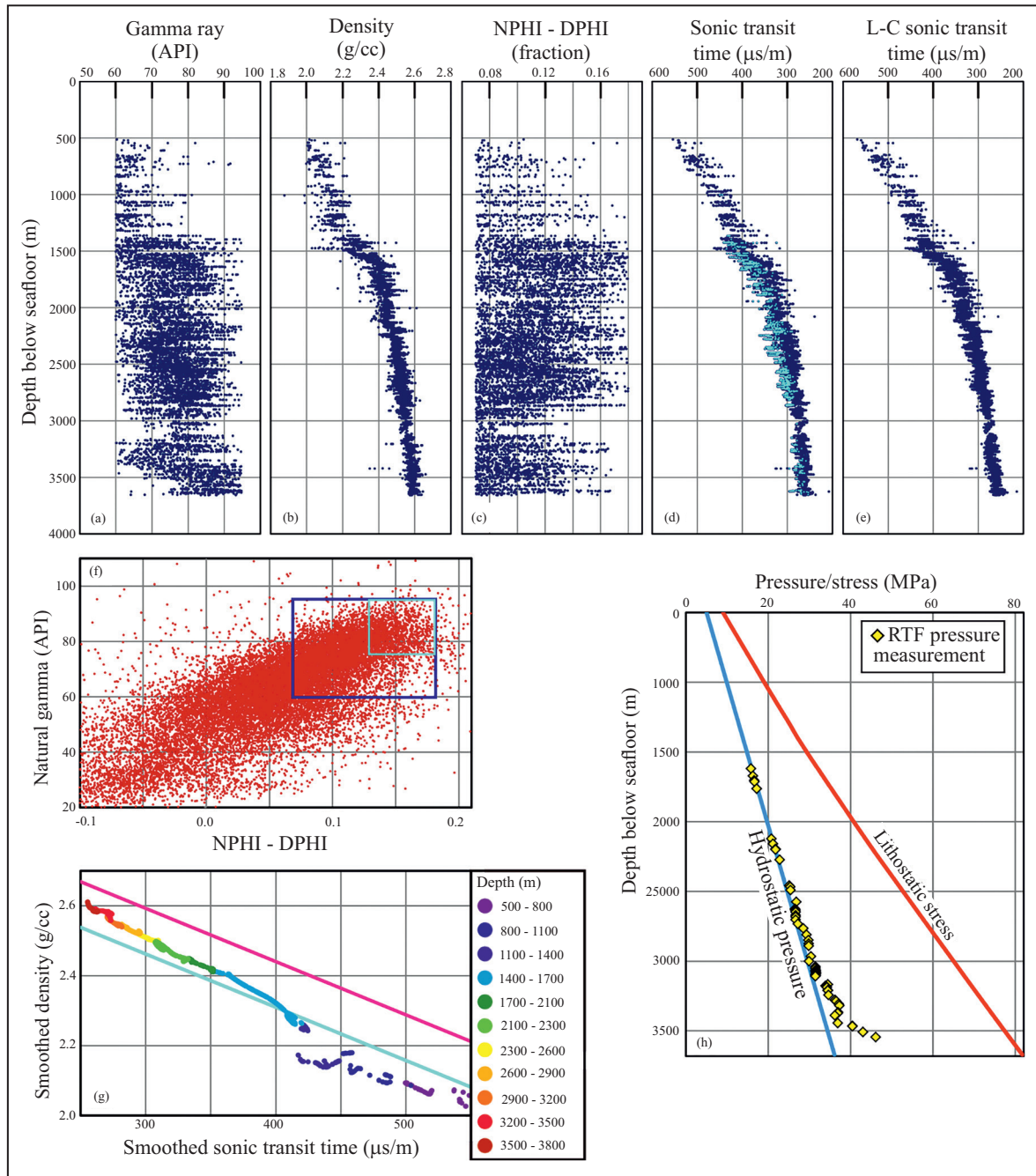


Figure 4. Wireline logs and derivatives from Well NWP-2. In (a)–(e) data are plotted for mudstone data points within the dark blue box marked on the crossplot in (f). (g) Crossplot of sonic transit time and density, apparently showing an early compaction trend for smectite-rich mudstones and a late compaction trend for illite-rich mudstones with a transition zone at ~1,400 m depth. (h) Pressure plot.

over the depth interval of 500 - 3,000 m subsea. Mudstones with higher clay fraction, as indicated by the cyan box in Figure 4f, tend to have greater sonic transit times (Figure 4d). Therefore corrections were calculated for the sonic log using the method described by Goultly *et al.* (2016) to yield the lithology corrected (L-C) sonic transit times plotted in Figure 4e.

### RESULTS AND DISCUSSIONS

The vertical stress was estimated from the full density logs, using offset wells for the shallower intervals as needed. Hydrostatic pressure was calculated for a pore fluid density of  $1.0 \text{ g cm}^{-3}$ . Hence, the vertical effective stress was estimated for each mudstone data point and the value of  $\beta$  was calculated from Equations 2 and 3 with  $\sigma'_0 = 107 \text{ MPa}$ .

The depth profile of  $\beta$  for mudstone data points in Well NWP-2, calculated using Equations 2 and 3, is plotted as the dark blue data points in Figure 5. The fraction of smectite was calculated from the seafloor downwards by the method of Dutta (2016), assuming that S/I transformation is a first-order kinetic reaction, and by the method of Cuadros (2006) through Equations 6 and 7c with  $K = 10^{-8} \text{ M}$  and  $S_0 = 1$ . The scale for smectite fraction at the bottom has been adjusted by linear regression of  $\beta$  on smectite fraction for the mudstone data points. This procedure scales the depth profile for smectite fraction optimally to demonstrate visually the good correlation between  $\beta$  and smectite fraction.

As a test on the suitability of choosing  $S_0 = 1$ , the calculation by the method of Cuadros (2006) was also done  $S_0 = 0.7$  with the result shown in the left panel of Figure 6. In this case, the effective potassium concentration  $K$  was selected to be  $9.18 \times [10]^{-9} \text{ M}$  to give  $S \approx 0.23$  at the temperature of  $120^\circ\text{C}$ . The fit of the calculated smectite fraction to the calculated values of beta for the mudstone data points is clearly inferior. Hence, all wells were analyzed with  $S_0 = 1$ .

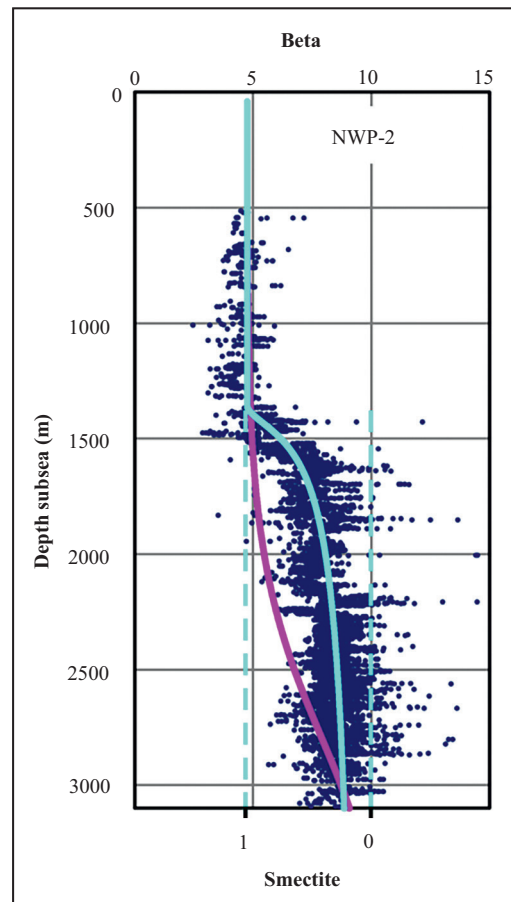


Figure 5. Plot of beta (dark blue data points) and relative proportion of smectite against depth in Well NWP-2. The relative proportion of smectite was calculated according to Dutta's parameters for a first-order kinetic reaction (magenta) and for a fifth-order reaction (cyan).

The depth profiles of  $\beta$  for all ten Peciko wells are plotted in Figure 7. The relative fraction of smectite was calculated from the seafloor downwards using Equations 6 and 7c with  $K = 10^{-8} \text{ M}$  (magenta curves in Figure 7). The scale for  $\beta$  at the top of Figure 5 is the same with the plots for all ten wells, whereas the scale for smectite fraction at the bottom has been adjusted by linear regression of  $\beta$  on smectite fraction for the mudstone data points. This procedure scales the depth profile for smectite fraction optimally to show its good correlation with  $\beta$ . In fact, the smectite fraction depth profiles are very similar in all wells, even though allowance was made for the different burial rates since 8 Ma (Lambert *et al.* 2003), ranging from  $279 \text{ m Ma}^{-1}$  to  $306 \text{ m Ma}^{-1}$  (Table 1).



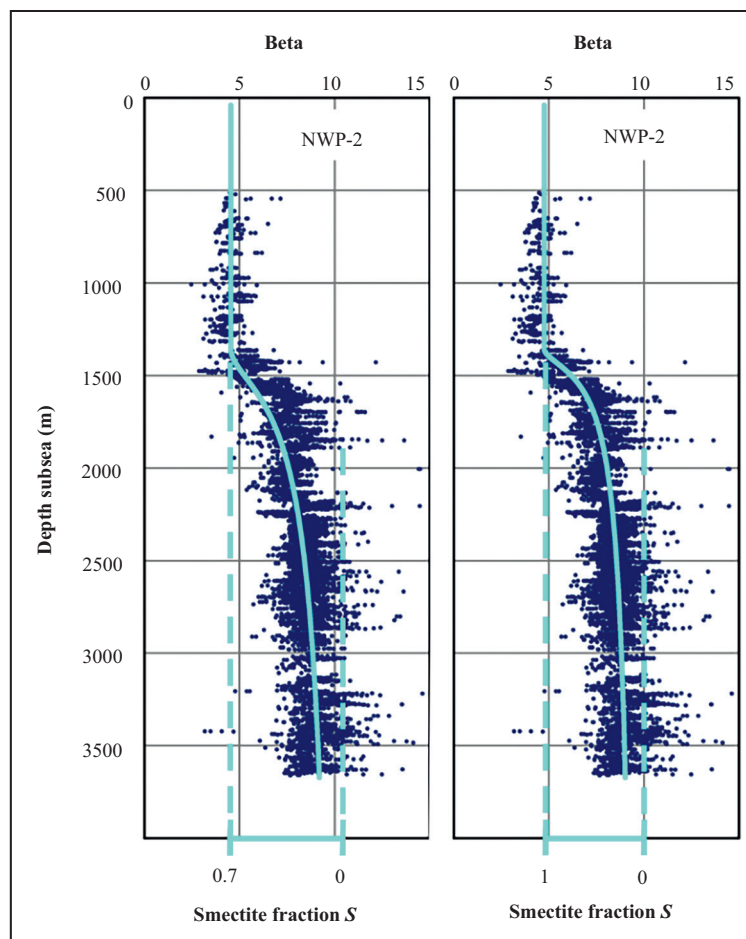


Figure 6. Plots of beta (dark blue data points) and relative proportion of smectite calculated for a fifth order reaction against depth. The initial smectite fraction is 0.7 in the plot on the left and 1.0 in the plot on the right.

The smectite fraction scale in Figure 7 had to be adjusted from one plot to the next because of discrepancies in the values of  $\beta$  between wells, which arose because of small-scale variations between density logs. The average mudstone density over the 500 - 3,000 m depth interval in well NWP-6 displays the greatest discrepancy, being approximately 1% greater than the mean mudstone density for all ten wells over the same depth interval. Consequently, the calculated values of void ratio in NWP-6 are relatively low, and the values of  $\beta$  are relatively high, reaching an average value of about 11 at 3,000 m depth compared to a more typical value around 9 in the other wells. This sensitivity of  $\beta$  to small discrepancies between density logs, whether due to calibration errors or to differences in the application of environmental corrections, would be

a serious concern when trying to estimate density normal compaction trends in overpressured wells. However, it does not impact the conclusion of this study, in which attention is limited to hydrostatically pressured mudstones where the vertical effective stress can be readily estimated.

The correlation between depth profiles for  $\beta$  and smectite fraction in each of the ten Peciko wells (Figure 7) is good, and the linear relationships between these two variables for each well are listed in Table 2. This result appears to support the idea that the Skempton-Dutta compaction relationship of Equation 1 is valid for mudstones throughout their transformation from smectite-rich to illite-rich composition. If so, the normal compaction trend for density through siliciclastic mudstones may be calculated from their temperature history with some local calibration for

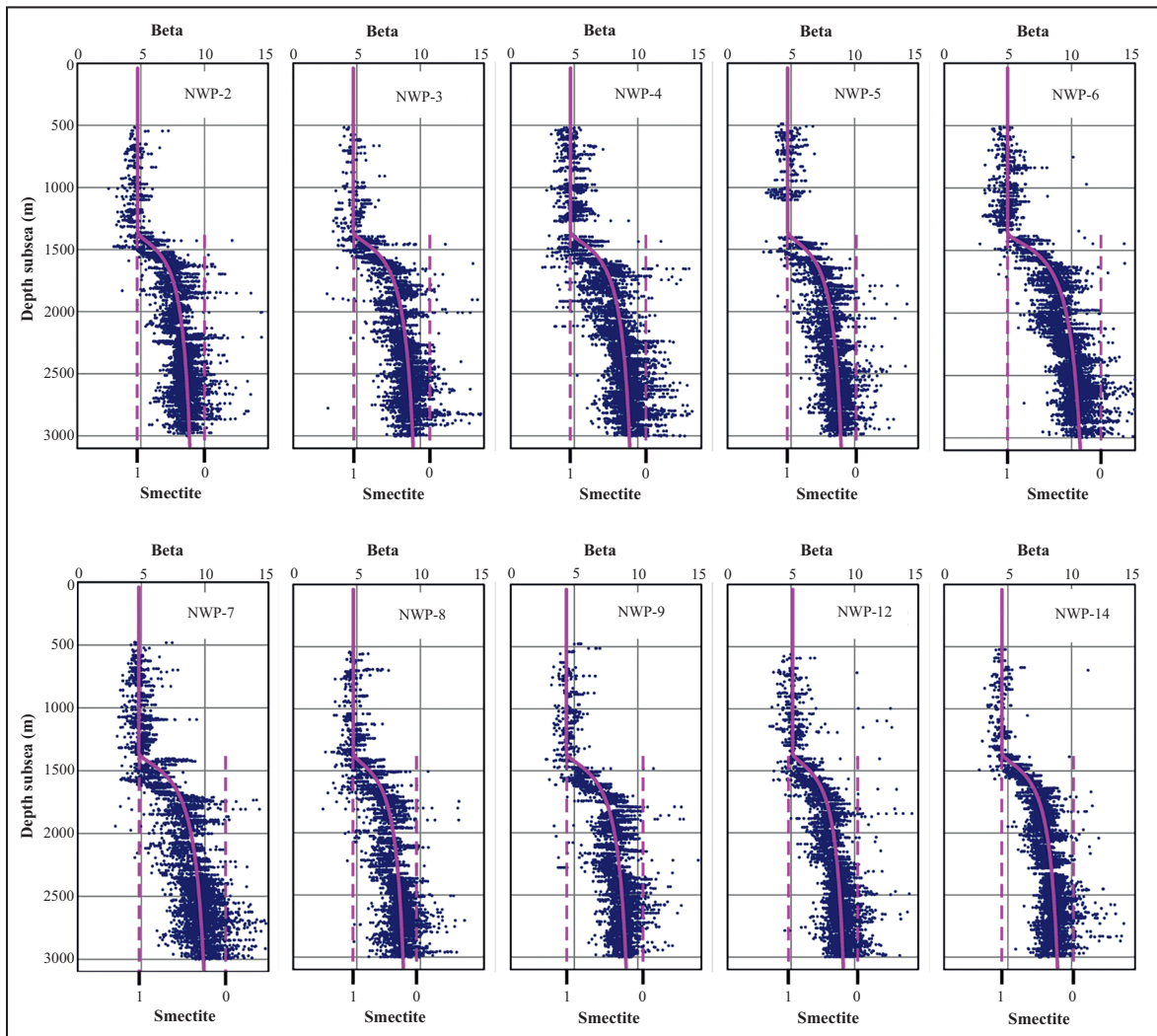


Figure 7. Plots of beta and relative proportion of smectite against depth. Values of beta are for selected mudstone data points only and plotted in dark blue. The relative proportion of smectite is plotted in magenta with the scale given on the bottom axis. The smectite scale is shifted and stretched against the beta scale for each well (*i.e.* a linear adjustment) to optimize the fit.

the effective potassium concentration ( $K$ ) and possibly for  $\sigma'_0$  and  $S_0$ .

Table 2. Linear Relationships between Beta ( $\beta$ ) and Smectite Fraction Determined for each of the Ten Peciko Wells

Well number	Linear relationship
NWP-2	$\beta = - 5.25S + 10.00$
NWP-3	$\beta = - 6.05S + 10.87$
NWP-4	$\beta = - 5.99S + 10.70$
NWP-5	$\beta = - 5.39S + 10.16$
NWP-6	$\beta = - 7.31S + 12.30$
NWP-7	$\beta = - 6.59S + 11.40$
NWP-8	$\beta = - 5.10S + 9.83$
NWP-9	$\beta = - 6.05S + 10.45$
NWP-12	$\beta = - 5.11S + 10.26$
NWP-14	$\beta = - 5.61S + 10.16$

The mudstone density normal compaction trends for the ten Peciko wells are shown in Figure 8. For each well, the smectite fraction over the depth range of 500 - 3,000 m subsea was calculated from Equations 6 and 7c with  $S_0 = 1.0$  and  $K = 10^{-8} M$ . Values of  $\beta$  for the mudstones in each well were found from the linear relationships between beta and smectite fraction in Table 2. Then, density values were calculated from Equations 1 - 3 with  $\sigma'_0 = 107$  MPa. The fit of the NCTs to the data is remarkably good, even below the top of overpressure, especially when one considers that each density NCT has been calculated from just two depth-dependent variables, the vertical effective stress and the smectite fraction.

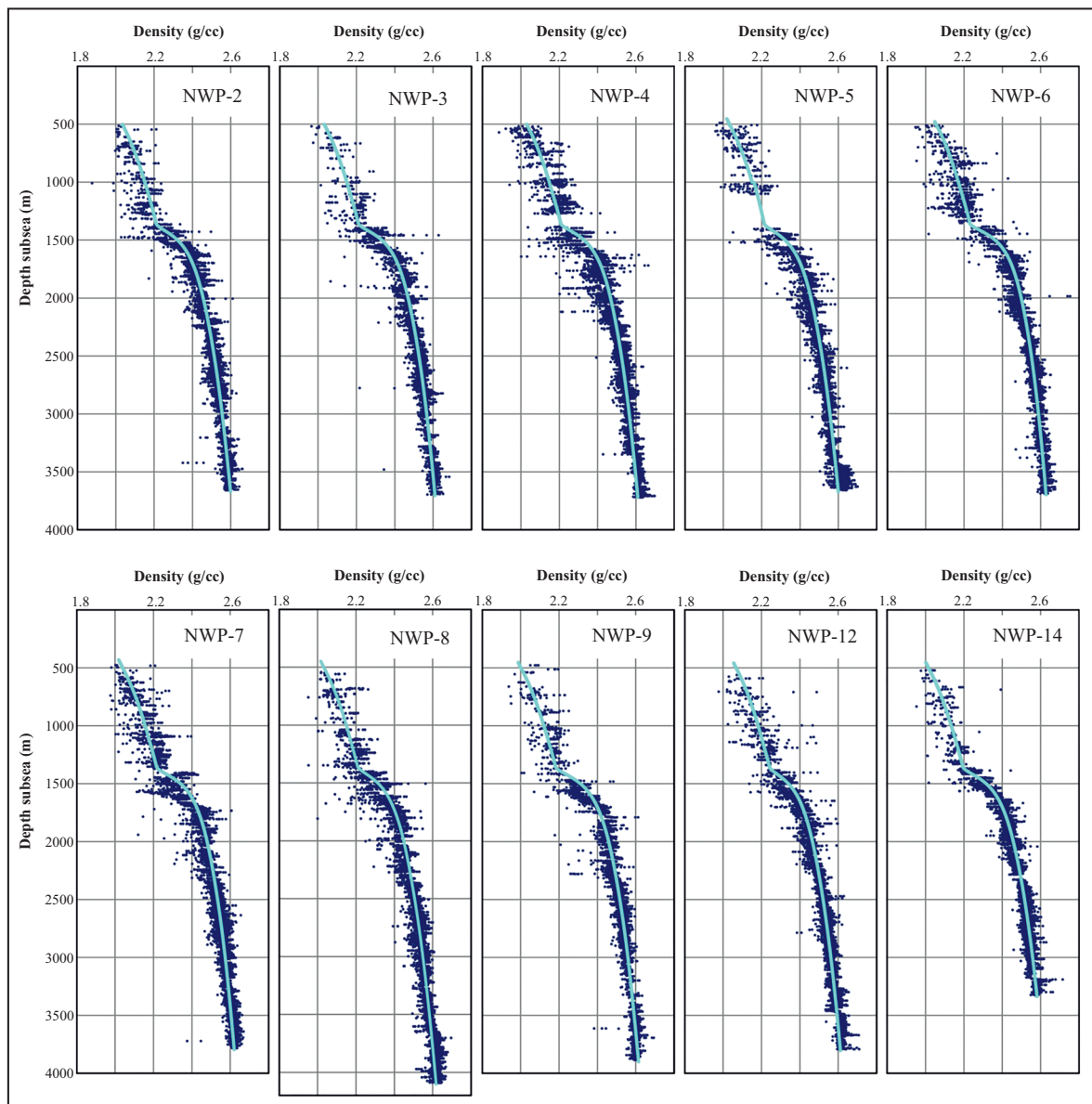


Figure 8. Density logs and normal compaction trends for mudstone data points in the ten Peciko wells.

### CONCLUSION

Our conclusion is that the correlation between depth profiles for  $\beta$  and smectite fraction in the ten plots is remarkably good. This result tends to confirm the idea that the Skempton-Dutta compaction relationship of Equation 1 is valid for mudstones throughout their transformation from smectite-rich to illite-rich composition. In principle, then, the normal compaction trend for density through siliciclastic mudstones may be calculated from their temperature history with

some local calibration, *e.g.* for the effective potassium concentration,  $K$ . The ability to calculate the density normal compaction trend would be useful for estimating pore pressure in overpressured wells using the two-step approach.

### ACKNOWLEDGEMENTS

The authors thank Total Indonesia for funding and data. However, the authors' views are not necessarily shared by Total Indonesia.

## REFERENCES

- Bjørlykke, K., 1998. Clay mineral diagenesis in sedimentary basins: a key to the prediction of rock properties: examples from the North Sea Basin. *Clay Minerals*, 33, p.15-34. DOI: 10.1180/claymin.1998.033.1.03.
- Boles, J.R. and Franks, S.G., 1979. Clay diagenesis in Wilcox sandstones of southwest Texas: implications of smectite diagenesis on sandstone cementation. *Journal of Sedimentary Petrology*, 49, p.55-70. DOI: 10.1306%2F2F12F76BC-2B24-11D7-8648000102C1865D.
- Chambers, J.L.C., Carter, I., Cloke, I.R., Craig, J., Moss, S.J., and Paterson, D.W., 2004. Thin-skinned and thick-skinned inversion-related thrusting – A structural model for the Kutai Basin, Kalimantan, Indonesia. In: McClay, K.R. (ed.), *Thrust Tectonics and Hydrocarbon Systems, American Association of Petroleum Geologist, Memoir*, 82, p.614-634. DOI: 10.1306/M82813C32.
- Clauer, N., Rinckenbach, T., Weber, F., Sommer, F., Chaudhuri, S., and O'Neil, J.R., 1999. Diagenetic evolution of clay minerals in oil-bearing Neogene sandstones and associated shales, Mahakam Delta Basin, Indonesia. *American Association of Petroleum Geologist, Bulletin*, 83, p.62-87. DOI: 10.1306/00AA9A02-1730-11D7-8645000102C1865D.
- Cloke, I.R., Moss, S.J., and Craig, J., 1999. Structural controls on the evolution of the Kutai Basin, East Kalimantan. *Journal of Asian Earth Sciences*, 17, p.137-156. DOI: 10.1016/S0743-9547(98)00036-1.
- Colten-Bradley, V.A., 1987. Role of pressure in smectite dehydration – Effects on geopressure and smectite-to-illite transformation. *American Association of Petroleum Geologist, Bulletin*, 71, p.1414-1427. DOI: 10.1306/703C8092-1707-11D7-8645000102C1865D.
- Cuadros, J., 2006. Modeling of smectite illitization in burial diagenesis environments. *Geochimica et Cosmochimica Acta*, 70, p.4181-4195. DOI: 10.1016/j.gca.2006.06.1372.
- Cuadros, J. and Linares, J., 1996. Experimental kinetic study of the smectite-to-illite transformation. *Geochimica et Cosmochimica Acta*, 60, p.439-453. DOI: 10.1016/00167037(95)00407-6.
- Dutta, N.C., 1986. Shale compaction, burial diagenesis and geopressures: a dynamic model, solution and some results. In: Burrus, J. (ed.), *Thermal Modeling in Sedimentary Basins*. p.149-172. Éditions Technip
- Dutta, N.C., 2016. Effect of chemical diagenesis on pore pressure in argillaceous sediment. *The Leading Edge*, 35, p.523-527. DOI: 10.1190/tle35060523.1.
- Elliot, W.C. and Matisoff, G., 1996. Evaluation of kinetic models for the smectite to illite transformation. *Clays and Clay Minerals*, 44, p.77-87. DOI: 10.1346/CCMN.1996.0440107.
- Goult, N.R., Sargent, C., Andras, P., and Aplin, A.C., 2016. Compaction of diagenetically altered mudstones - Part 1. Mechanical and chemical contributions. *Marine and Petroleum Geology*, 77, p.703-713.
- Hall, R., 2009. Hydrocarbon basins in SE Asia: understanding why they are there. *Petroleum Geoscience*, 15, p.131-146. DOI:10.1144/1354-079309-830.
- Hower, J., Eslinger, E.V., Hower, M.E., and Perry, E.A., 1976. Mechanism of burial and metamorphism of argillaceous sediment: 1. Mineralogical and chemical evidence. *Geological Society of America Bulletin*, 87, p.725-737. DOI: 10.1130/0016-7606(1976)87%3C725:MOBMOA%3E2.0.CO;2.
- Lambert, B., Duval, B.C., Grosjean, Y., Umar, I.M., and Zaugg, P., 2003. The Peciko case history: impact of an evolving geological model on the dramatic increase of gas reserves in the Mahakam Delta. In: Halbouty, M.T. (ed.), *Giant Oil and Gas Fields of the Decade 1990–1999*. AAPG, 78, p.297-320. DOI: 10.1306/M78834C17.
- Ramadhan, A.M. and Goult, N.R., 2010. Overpressure generating mechanisms in the Peciko Field, Kutai Basin, Indonesia. *Petroleum Geoscience*, 16, p.367-376. DOI: 10.1144/1354-079309-027.

- Ramdhan, A.M. and Goultly N.R., 2011. Overpressure and mudrock compaction in the Lower Kutai Basin, Indonesia: A radical reappraisal. *American Association of Petroleum Geologist, Bulletin*, 95, p.1725-1744. DOI: 10.1306/02221110094.
- Ramdhan, A.M. and Goultly, N.R., 2018. Two-step wireline log analysis of overpressure in the Bekapai Field, Lower Kutai Basin, Indonesia. *Petroleum Geoscience*, 24 (2), p.208-217. DOI: 10.1144/petgeo2017-045.
- Robertson, H.E. and Lahann, R.W., 1981. Smectite to illite conversion rates. Effect of solution chemistry. *Clays and Clay Minerals*, 29, p. 129-135. <http://dx.doi.org/10.1346/CCMN.1981.0290207>.
- Samson, P., Dewi-Rochette, T., and Lescoeur, M., 2005. Peciko geological modeling: optimizing fluid distribution and model resolution of a giant gas field in a shale-dominated deltaic environment. *Asia Pacific Oil & Gas Conference*, SPE paper 93253. DOI: 10.2118/93253-MS.
- Skempton, A.W., 1969. The consolidation of clays by gravitational compaction. *Quarterly Journal of the Geological Society*, 125, p.373-411. DOI: 10.1144/gsjgs.125.1.0373.
- Total E&P Indonesie, 2000. Stratigraphic column of the Lower Kutai Basin. Unpublished Report.